Inorganic Chemistry

Article

pubs.acs.org/IC

Dynamic Magnetic Materials Based on the Cationic Coordination Polymer $[Cu(btix)_2]_n^{2n+}$ [btix = 1,4-Bis(triazol-1-ylmethyl)benzene]: Tuning the Structural and Magnetic Properties through Anion Exchange

Eugenio Coronado, Mónica Giménez-Marqués, Carlos J. Gómez-García, and Guillermo Mínguez Espallargas*

Instituto de Ciencia Molecular (ICMol), Universidad de Valencia, c/Catedrático José Beltrán 2, 46980 Paterna, Spain

Supporting Information

ABSTRACT: A three-dimensional coordination polymer, $[Cu(btix)_2(BF_4)_2]_n$ [btix = 1,4-bis(triazol-1-ylmethyl)benzene], with antiferromagnetic interactions occurring via the organic ligand, has been prepared and characterized. It has been shown to permit the exchange of anionic species in the crystalline network with modification of the magnetic properties. Coordinated BF_4^- can be reversibly exchanged by different anions with (NO_3^- and Cl^-) or without (PF_6^- and ClO_4^-) dynamic response of the organic ligand, which acts as the only linker between the metal centers. Interestingly, an irreversible exchange occurs with N_3^- anions to generate a new coordination polymer, $[Cu(btix)(N_3)_2]_n$, whose structure has been determined ab initio by powder X-ray diffraction, revealing a totally different connectivity between the Cu^{II} centers. These structural transformations are accompanied by a change of the magnetic properties, which have been detected by electron paramagnetic resonance and magnetic susceptibility measurements.

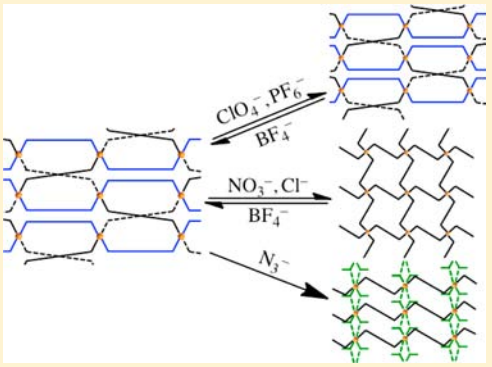

INTRODUCTION

Responsive magnetic materials are an important class of materials where the magnetic properties can be modified by structural changes provoked by an external stimulus, making them suitable candidates for potential application as switches or sensors.[1] Coordination polymers, composed of metal ions or clusters connected by organic ligands into crystalline networks,[2−4] are ideal systems for the design of these magnetic tunable materials.[5] Physical stimuli such as light and pressure have been extensively used to reversibly change the magnetic properties at low temperatures,[6] whereas the use of chemical stimuli for this purpose is less common.[7] In fact, chemical postsynthetic modification of extended metal−organic frameworks (MOFs) is currently attracting much attention,[4h,8] although it is mainly focused on modification of the organic ligands with minor changes in the connectivity of the metal centers, for which examples are scarce.[9]

An extensively studied noncovalent postsynthetic modification of coordination polymers consists of ion exchange,[10] which has been shown as an effective way to tune gas sorption[11] and for anion recognition in more complex smart materials.[12] Most commonly, the ions are trapped in the pores and are weakly bonded to the (ionic) framework. In these cases, ion exchange can occur in a single-crystal-to-single-crystal manner because noncoordinated ions can be easily exchanged without massive perturbation of the network. However, anion exchange involving metal-coordinated anions[13] often yields a poorly crystalline powder since the cleavage and formation of coordination bonds can provoke breaks in the crystals. Here we report a nonporous coordination polymer in which the flexibility provided by the organic ligand allows the exchange of coordinated BF_4^- anions with different anions. Interestingly, even if the structural changes that accompany this anion exchange are profound, the crystallinity of the solid is maintained. In fact, three different types of dynamic response of the organic bridge between the metal centers are observed: (i) retention of the configuration of the organic ligand with no major structural changes; (ii) switch of the configuration of the organic ligand with a reduction of the dimensionality of the network; and (iii) switch of the configuration of the organic ligand with a complete rearrangement of the structure. As these structural changes affect the connectivity between the metal centers, their magnetic properties also change. These features open the possibility of using these materials for the trapping and sensing of anions.

EXPERIMENTAL SECTION

All reagents and solvents were commercially available and used without further purification. The ligand 1,4-bis(triazol-1-ylmethyl)-benzene (btix) was prepared according to a literature method.[14]

Received: September 24, 2012
Published: November 13, 2012

   dx.doi.org/10.1021/ic302066e | Inorg. Chem. 2012, 51, 12938−12947

Synthesis of *trans*-$[Cu(btix)_2(BF_4)_2]_n$ (1). A solution of btix (321 mg, 1.3 mmol) in 50 mL of methanol (MeOH) was added dropwise into a methanolic solution of $Cu(BF_4)_2{\cdot}xH_2O$ (175 mg) without stirring. The mixture was left at room temperature for crystallization. After several hours, light-purple block-shaped crystals suitable for X-ray crystallography were filtered off and washed with MeOH. Phase purity was established by powder X-ray diffraction (PXRD). Yield: 87%. Anal. Calcd for $C_{24}H_{24}CuN_{12}B_2F_8$ (717.68): C, 40.17; H, 3.37; N, 23.42. Found: C, 38.54; H, 3.42; N, 22.41. FT-IR (KBr pellet, cm^{-1}): 3144 (s), 1532 (vs), 1443 (m), 1427 (s), 1346 (w), 1292 (m), 1125 (vs), 1083 (vs), 1115 (vs), 991 (vs), 897 (m), 766 (m), 732 (m), 676 (s), 520 (m).

Anion Exchange. Powdered samples of **1** (50 mg) were each immersed in aqueous solutions of $NaClO_4$, $NaPF_6$, $NaNO_3$, NaCl, or NaN_3 (3 M, 5 mL) and left for 1 day, although a color change is observed within seconds. The resulting anion-exchanged solids **2**–**6** [exchanged with ClO_4^- (**2**), PF_6^- (**3**), NO_3^- (**4**), Cl^- (**5**), and N_3^- (**6**)] were collected by centrifugation, washed several times with water, and vacuum dried. The products were characterized by elemental analysis (EA), Fourier-transformed infrared spectroscopy (FT-IR), and PXRD. To verify the reversibility of the process, the anion-exchanged solids were immersed in 3 M $NaBF_4$ for 1 day, collected by centrifugation, washed several times with water, and vacuum dried. All solids were characterized by FT-IR and PXRD.

Single-Crystal X-ray Diffraction. A single crystal of compound **1** was mounted on a glass fiber using a viscous hydrocarbon oil to coat the crystal and then transferred directly to the cold nitrogen stream for data collection. X-ray data were collected at 120 K on a Supernova diffractometer equipped with a graphite-monochromated enhanced (Mo) X-ray source (λ = 0.71073 Å). The program *CrysAlisPro*, Oxford Diffraction Ltd., was used for unit cell determinations and data reduction. Empirical absorption correction was performed using spherical harmonics, implemented in the *SCALE3 ABSPACK* scaling algorithm. The crystal structure was solved and refined against all F^2 values using the *SHELXTL* suite of programs.[15] Non-hydrogen atoms were refined anisotropically (except the disordered fragments), and hydrogen atoms were placed in calculated positions, refined using idealized geometries (riding model), and assigned fixed isotropic displacement parameters except for those of water molecules, which were located and refined with distance restraints. In **1**, the benzene moiety of the *syn*-btix ligand is disordered over two sites and modeled with a 50:50 ratio. A summary of the data collection and structure refinements is provided in Table 1.

PXRD. A polycrystalline sample of **6** was lightly ground in an agate mortar and pestle and filled into a 0.3 mm glass boron capillary prior to being mounted and aligned on a Empyrean PANalytical powder diffractometer, using Cu Kα_1 radiation (λ = 1.54177 Å). A total of 35 repeated measurements were collected at room temperature (2θ = 3–70°) and merged in a single diffractogram. The diffraction pattern was indexed using *TOPAS*[16] to a monoclinic cell, and space group *C*2/*c* was assigned from volume considerations and a statistical consideration of the systematic absences. The data set was background-subtracted and truncated to d = 2.885 Å (2θ = 31.00°), for Pawley refinement[17] and structure solution using the simulated-annealing (SA) global optimization procedure, described previously,[18] which is now implemented in the *DASH* computer program.[19] The SA structure solution involved optimization of three independent fragments in the asymmetric unit (half of a copper atom, half of a btix ligand, and one azido ligand, considered from the composition of compound **6**), totalling 19 degrees of freedom. **Z** matrices describing the molecular topology of the fragments were generated automatically within *DASH* using analogous moieties taken from the CSD. Global optimization of all external (rotational and translational) degrees of freedom against the extracted intensities was carried out with all *DASH* SA control parameters set to default values. A total of 10 runs with 5×10^7 SA moves per run were implemented for each structure determination. The best SA solutions had a chemically reasonable packing arrangement and exhibited no significant misfit to the data. The solved structure was used as a starting model for Rietveld refinement,[20] conducted using *TOPAS*. All atomic positions and displacement parameters, U_{iso}, of non-hydrogen atoms were refined (one for the copper atom and one for all carbon and nitrogen atoms; hydrogen atoms were fixed at idealized positions, and the atomic displacement parameters were set as 1.2 times those of non-hydrogen atoms), subject to a series of restraints on the bond lengths, bond angles, and planarity of the aromatic rings. A March-Dollase correction of the intensities for the preferred orientation was applied in the final stage of refinement. The observed and calculated diffraction patterns for the refined crystal structures are shown in Figure 3. The Rietveld refinement converged to R_{wp} = 0.0504 and R_{wp}' = 0.14426 (R_{wp}' is the background-subtracted R_{wp}; Table 2).

Table 1. Crystallographic Data for Compound 1

compound	**1**
empirical formula	$C_{24}H_{24}N_{12}B_2F_8Cu$
fw	717.71
cryst color	purple
cryst size (mm^3)	0.15 × 0.15 × 0.05
temperature (K)	120(2)
cryst syst, Z	monoclinic, 4
space group	*C*2/*c*
a (Å)	23.820(9)
b (Å)	9.5063(15)
c (Å)	15.544(6)
α (deg)	90.00
β (deg)	123.97(6)
γ (deg)	90.00
V ($Å^3$)	2918.8(16)
ρ_{calc} ($Mg{\cdot}m^{-3}$)	1.633
μ(Mo Kα) (mm^{-1})	0.840
θ range (deg)	2.38–25.03
reflns collected	6214
indep reflns (R_{int})	2576 (0.1448)
reflns used in refinement, n	2576
LS parameters, p/restraints, r	212/0
R1(F),[a] $I > 2\sigma(I)$	0.0763
wR2(F^2),[b] all data	0.1510
$S(F^2)$,[c] all data	0.973

[a] $R1(F) = \sum(|F_o| - |F_c|)/\sum|F_o|$. [b] $wR2(F^2) = [\sum w(F_o^2 - F_c^2)^2/\sum wF_o^4]^{1/2}$. [c] $S(F^2) = [\sum w(F_o^2 - F_c^2)^2/(n + r - p)]^{1/2}$.

CCDC 895356 (**1**) and 895357 (**6**) contain the supplementary crystallographic data for this paper. These data can be obtained free of charge from The Cambridge Crystallographic Data Centre via www.ccdc.cam.ac.uk/data_request/cif. See also the Supporting Information.

Phase purity of polycrystalline samples of **1**–**5** was established by PXRD. Polycrystalline samples of **1**–**5** were lightly ground in an agate mortar and pestle and filled into 0.5 mm borosilicate capillaries. Data were collected at room temperature in the 2θ range 2–50° on a Empyrean PANalytical powder diffractometer, using Cu Kα radiation (λ = 1.54177 Å). Pawley refinements[17] were performed using the *TOPAS* computer program[16] and revealed an excellent fit to a one-phase model for compounds **1** (R_{wp} = 0.0322; GOF = 1.812; Figure 2a), **2** (R_{wp} = 0.0284; GOF = 1.606; Figure 2b), **3** (R_{wp} = 0.0368; GOF = 2.006; Figure 2c), **4** (R_{wp} = 0.0475; GOF = 2.751; Figure 2d), and **5** (R_{wp} = 0.0235; GOF = 2.438; Figure 2e), indicating the absence of any other detectable crystalline phases. In all cases, the unit cell obtained from the Pawley refinement is consistent with those obtained for analogous structures by single-crystal diffraction (see the Supporting Information).

Magnetic Measurements. Magnetic susceptibility measurements were performed on single-phased polycrystalline samples of **1** and **4**–**6** with a Quantum Design MPMS-XL-5 SQUID susceptometer. The susceptibility data were corrected from the diamagnetic contributions as deduced by using Pascal's constant tables. The susceptibility data were collected in the range 2–300 K with an applied field of 0.1 T. Field dependences of the magnetization were measured at 2.0 K.

dx.doi.org/10.1021/ic302066e | *Inorg. Chem.* 2012, 51, 12938–12947

Table 2. Data Collection, Structure Solution, and Refinement Parameters of Compound 6

compound	**6**
empirical formula	$C_{12}H_{12}N_{12}Cu$
fw	387.89
specimen color	green
specimen shape (mm^3)	cylinder, 12 × 0.7 × 0.7
wavelength, λ (Å)	0.71073
cryst syst	monoclinic
space group, Z	$C2/c$, 4
a (Å)	24.4913(10)
b (Å)	4.34232(12)
c (Å)	14.20752(55)
α (deg)	90
β (deg)	78.885(3)
γ (deg)	90
V ($Å^3$)	1482.61(9)
density ($Mg·m^{-3}$)	1.737
temperature (K)	298
μ (mm^{-1})	2.329
2θ range (deg)	3.0−70.0
increment in 2θ (deg)	0.014
reflns measd, n	331
specimen mounting	0.7 mm borosilicate capillary
mode	transmission
detector	PIXcel
param refined, p	94
restraints, r	36
R_p[a]	0.0386
R_{wp}[b]	0.0504
R_{exp}[c]	0.0377
GOF,[d] all data	1.320

[a] $R_p = \sum|y_o - y_c|/\sum y_o$. [b] $R_{wp} = [\sum w(y_o - y_c)^2/\sum w(y_o)^2]^{1/2}$. [c] $R_{exp} = R_{wp}/GOF$. [d] $GOF = [\sum w(y_o - y_c)^2/(n - p + r)]^{1/2}$.

Electron paramagnetic resonance (EPR) spectroscopy were recorded with a Bruker ELEXYS E580 spectrometer operating in X band (9.47 GHz) in the temperature range 4−300K.

RESULTS

Crystal Structure of 1. The reaction of $Cu(BF_4)_2·xH_2O$ and btix in MeOH results in the formation of block-shaped crystals of **1**.[21] Single-crystal X-ray analysis of compound **1** reveals that it is composed of a three-dimensional (3D) network that crystallizes in the monoclinic $C2/c$ space group (Figure 1). In this coordination polymer, the ligand adopts two different conformations, syn and anti. The asymmetric unit contains one crystallographically independent Cu^{II} ion, two btix ligands, and two coordinated BF_4^- anions. Each metal is coordinated by four triazole nitrogen atoms derived from two *syn*-btix and two *anti*-btix ligands in the equatorial positions and two fluorine atoms from two BF_4^- anions in the apical positions. The coordination environment of the Cu^{II} ions features a slightly distorted octahedron with Cu−N distances of 2.006(6) and 2.000(6) Å and a longer Cu−F distance of 2.422(5) Å, as a result of the Jahn−Teller elongation along the Cu−F bonds and of the weak coordination ability of this anion.[22] The bond angles slightly deviate from the idealized octahedral geometry (see Table 3). All btix ligands act as bridges between adjacent metal centers, leading to Cu···Cu distances of 9.940(17) and 14.112(11) Å. A remarkably important feature is the presence of Cu−FBF_3 coordination bonds in **1**. The BF_4^- anion is commonly used as a noncoordinated anion;[22] its coordination ability index, a (transition metal),[23] is −1.1, indicative of a poor tendency to coordinate. Interestingly, each copper center is bonded to two different BF_4^- anions in trans positions. The 3D structure can be described as chains further linked in the other two directions. The *syn*-btix ligands link the copper centers, forming an undulating chain along the [10−1] direction (see Figure 1b), which is connected to four neighboring chains via the *anti*-btix ligands in an alternating fashion: each copper center of the undulating chain is connected to two chains, but two consecutive copper centers do not connect the same two chains (see Figure 1c,d).

Anion Exchange. Powder samples of **1** were immersed at room temperature for 1 day in 3 M aqueous solutions containing $NaClO_4$, $NaPF_6$, $NaNO_3$, NaCl, or NaN_3. The BF_4^- anion in **1** was quantitatively exchanged with ClO_4^- (**2**), PF_6^- (**3**), NO_3^- (**4**), Cl^- (**5**), and N_3^- (**6**) accompanied by a color change from purple to different blues for polymers **2**−**5** and a remarkable color change to dark green in polymer **6**. All products **2**−**6** were identified by EA, FT-IR, and PXRD. EA provides information about the stoichiometry of the exchanged products. Thus, compounds **2**−**5** show a 1:2:2 ratio for Cu/btix/anion, whereas this ratio is 1:1:2 for compound **6** (see the Supporting Information). In the FT-IR spectra of products **2**−**6**, new stretching vibrations corresponding to ClO_4^- (1105−1120 and 623 cm^{-1}), PF_6^- (839 and 558 cm^{-1}), NO_3^- (1384−1337 cm^{-1}), Cl^- (3110−3091 and 637 cm^{-1}), and N_3^- (2046 and 2025 cm^{-1}) clearly appear, while the peak associated with BF_4^- (1084 cm^{-1}) disappears, indicating that the anion exchange is total (see the Supporting Information).[24] Finally, PXRD studies show that the crystallinity of **1** is retained during the exchange processes and establish that the anion substitution strongly determines the final structure (see Figure 2). Thus, the exchanged polymers **2**−**6** can be classified into three different categories depending on the structural transformations that occurred during the anion exchange: (i) retention of the framework in polymers **2** and **3**, whose PXRD patterns match those of the original polymer **1**, indicating that the skeletal structure of the polymer remains stable upon anion exchange; (ii) reduction of the dimensionality in polymers **4** and **5**, which show PXRD patterns similar to the 2D polymer *trans*-$[Cu(btix)_2Cl_2]_n$ and *trans*-$[Co(btix)_2(NO_3)_2]_n$ previously reported;[21,25] (iii) complete rearrangement of the network in polymer **6**, whose PXRD pattern suggests a totally different structure than the original network **1**.

The reversibility of the anion exchange has been examined by immersion of the exchanged products in 3 M $NaBF_4$ for 1 day. The ClO_4^-, PF_6^-, and Cl^- anions in polymers **2**, **3**, and **5**, respectively, were quantitatively exchanged with BF_4^- and therefore reconverted into **1**. However, the NO_3^- anion in **4** was only partially exchanged even when the solid was immersed in a 3 M $NaBF_4$ solution for 3 days, as confirmed by FT-IR. As expected, reversibility is unfeasible for polymer **6**, likely because of the strength of the coordinating anion. The results are summarized in Scheme 1.

Crystal Structure of 6. An ab initio solution from PXRD data and Rietveld refinement (Figure 3) show that compound **6** consists of a two-dimensional (2D) network that crystallizes in the monoclinic space group $C2/c$. The asymmetric unit contains one crystallographically independent Cu^{II} located at the 2-fold axis, half *anti*-btix bridging ligand, and one coordinated N_3^- anions with an asymmetric end-on (1,1′)

dx.doi.org/10.1021/ic302066e | Inorg. Chem. 2012, 51, 12938−12947

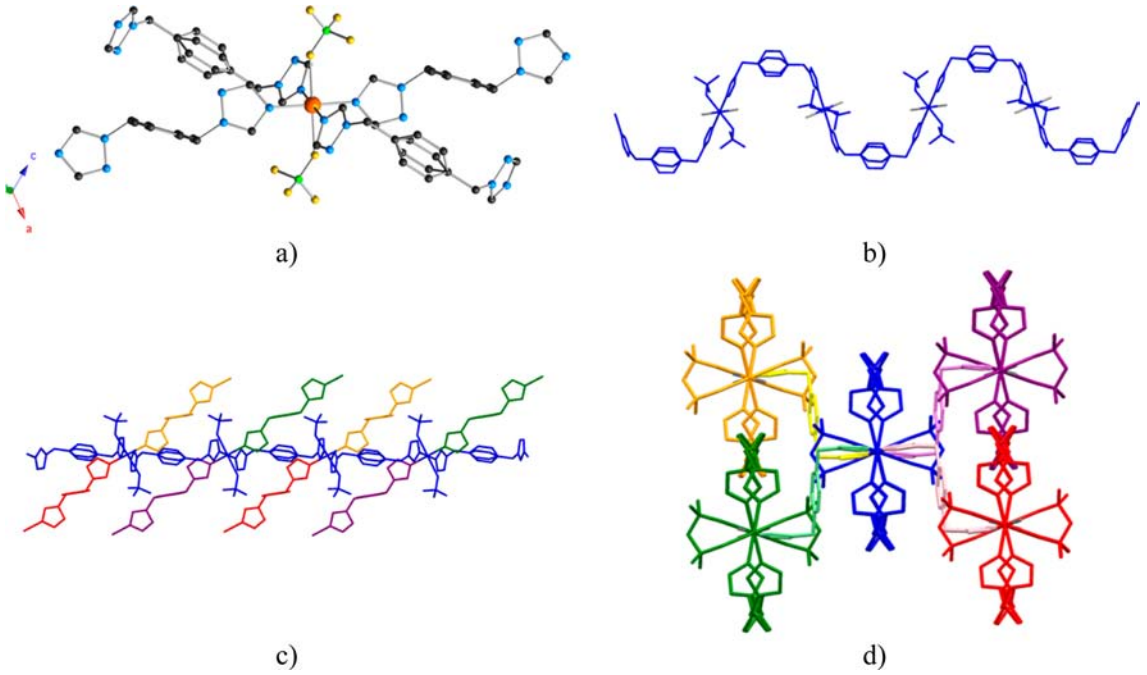

Figure 1. (a) Coordination environment of the Cu^{II} centers in **1**, showing the connection to two *syn*-btix, two *anti*-btix, and two BF_4^- anions (copper, nitrogen, carbon, boron, and fluorine are colored orange, blue, black, green, and yellow, respectively). (b) Undulating chain along the [10−1] direction formed by *syn*-btix ligands. (c) Top view of the undulating chain (in blue) showing the *anti*-btix ligands that connect with four adjacent chains (colors of the *anti*-btix refer to the colors of the different undulating chains in part d to which they connect). (d) Front view of the central chain (in blue) and its four adjacent chains (in red, violet, green, and yellow). Hydrogen atoms have been omitted in all figures for clarity.

Table 3. Selected Bond Lengths (Å) and Angles (deg) for 1 and 6

	1		6
Cu−N	2.006(6)	$Cu-N_{az}$	2.036(10)
	2.000(6)		2.886(10)
Cu−F	2.422(5)	$Cu-N_{btix}$	2.079(5)
N−Cu−N	91.90(22)	$N_{az}-Cu-N_{btix}$	96.2(3)
	88.10(22)		81.9(3)
N−Cu−F	93.73(21)		
	89.99(20)		
F−Cu−F	180		

bridging mode resulting in a neutral 2D network (Figure 4). The metal environment is distorted octahedral: the basal plane is formed by four nitrogen atoms from two coordinated and two semicoordinated azidos, whereas the axial positions are filled by two triazole nitrogen atoms derived from two *anti*-btix (see Table 3).

The $Cu-N_{btix}$ bond length [2.079(5) Å] is similar to those reported for other btix-containing Cu^{II} complexes.[21,26a] The values of the equatorial $Cu-N_{az}$ are 2.036(10) and 2.886(10) Å for coordinated and semicoordinated azidos, respectively, indicating an asymmetric azido bridge, which leads to a Cu···Cu distance of 4.342(8) Å within this chain. The $Cu-N_{az}-Cu$ angle is 122.9(4)°. The azido groups in **6** are essentially linear with a N−N−N bond angle of 179.8(10)°. The two N−N bond distances within the azido groups are significantly different [1.095(10) and 1.113(11) Å], with the longer bond involving the end that is coordinated to the metal ion, as expected. The *anti*-btix ligand acts as a bridge between adjacent metal centers, leading to a Cu···Cu distance of 15.3338(9) Å and forming a 2D layer parallel to the (101) plane.

Magnetic Properties. The products of the molar magnetic susceptibility times the temperature, $\chi_m T$, per Cu^{II} ion for compounds **1** and **4**−**6** are shown in Figure 5. At room temperature, $\chi_m T$ has a value of 0.45 $cm^3 \cdot K \cdot mol^{-1}$ for **1**, close to the expected value for an isolated $S = {}^1/_2$ Cu^{II} ion with a g factor of ca. 2.19 (Figure 5a). When the temperature is decreased, $\chi_m T$ remains constant down to ca. 10 K, where it rapidly decreases, reaching a value of 0.14 $cm^3 \cdot K \cdot mol^{-1}$ at 2 K. The $\chi_m T$ products for **4** and **5** are very similar: they show a room temperature value per Cu^{II} ion of ca. 0.45 $cm^3 \cdot K \cdot mol^{-1}$, which remains constant down to very low temperatures and then shows a smooth decrease, which is more abrupt in **5** than in **4** (Figure 5c,d). At 2 K, the $\chi_m T$ values are ca. 0.42 and 0.38 $cm^3 \cdot K \cdot mol^{-1}$ for **4** and **5**, respectively. The $\chi_m T$ product of compound **6** shows a similar value at room temperature (ca. 0.45 $cm^3 \cdot K \cdot mol^{-1}$; Figure 5d), but below ca. 100 K, $\chi_m T$ increases upon further cooling to reach a maximum of ca. 1.06 $cm^3 \cdot K \cdot mol^{-1}$ at ca. 3 K (inset in Figure 5d).

The decrease observed in $\chi_m T$ for compound **1** indicates the presence of very weak antiferromagnetic Cu−Cu interactions that, given the structure of this compound, have to occur through the btix bridges connecting the Cu^{II} ions. As was already explained in the description of the structure, we can consider that this compound is formed by regular Cu^{II} chains, where the Cu^{II} ions are connected through equivalent *syn*-btix ligands (blue undulating chains in Figure 1). These chains are further connected with four equivalent chains via additional *anti*-btix ligands although in an alternating way (one copper atom is linked to chains A and B, and the following copper atom is linked to chains C and D). Accordingly, in order to fit the magnetic properties of compound **1**, we have used a simple $S = {}^1/_2$ antiferromagnetic regular chain (J) model[27] plus an

dx.doi.org/10.1021/ic302066e | Inorg. Chem. 2012, 51, 12938−12947

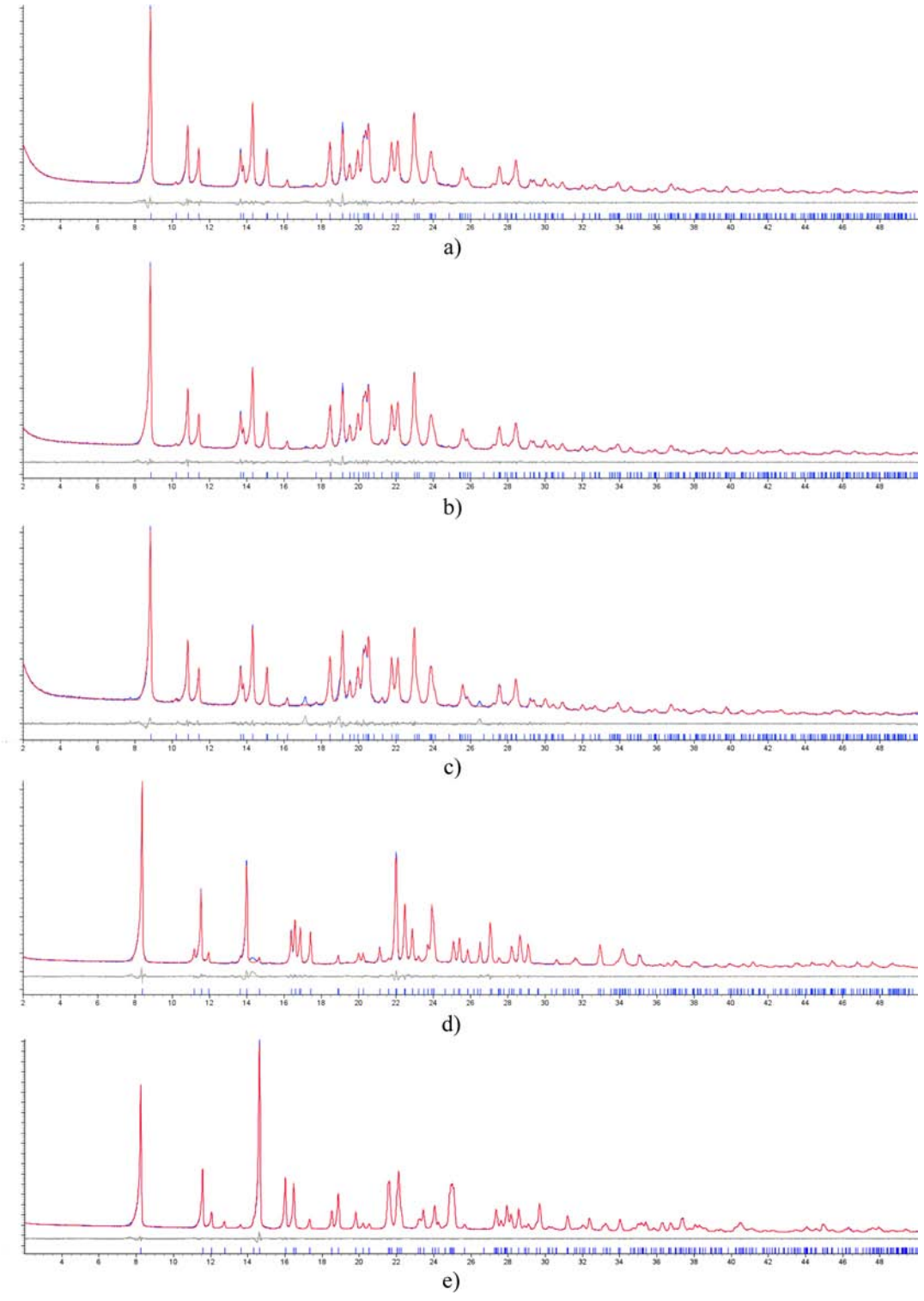

Figure 2. Observed (blue) and calculated (red) profiles and difference plots ($I_{obs} - I_{calcd}$; gray) of the Pawley refinements (2θ range 2.0−50.0°; maximum resolution 1.82 Å) for compounds (a) **1**, (b) **2**, (c) **3**, (d) **4**, and (e) **5**.

additional interchain interaction (zj, with $z = 4$), modeled with the molecular-field approximation.[28] This simple model reproduces very satisfactorily the magnetic properties of compound **1** in the whole temperature range with $g = 2.20$, $J = -4.1$ cm^{-1}, and $j = -1.1$ cm^{-1} (solid line in Figure 5a, with the Hamiltonian written as $H = -J\sum S_i S_{i+1}$). As expected, both exchange constants are weak and antiferromagnetic. Note that, although the two exchange constants are weak, we can assume that the *syn*-btix bridges yield a larger coupling constant, whereas the *anti*-btix ones should provide a weaker coupling, in agreement with the proposed model.

The magnetic behavior observed for compounds **4** and **5** indicates that both compounds are essentially paramagnetic with a very weak antiferromagnetic interaction between the Cu^{II} ions. Because both compounds present a 2D array of Cu^{II} ions with two equivalent bridges in both directions inside the

dx.doi.org/10.1021/ic302066e | *Inorg. Chem.* 2012, 51, 12938−12947

Scheme 1. Different Transformations upon Anion Exchange

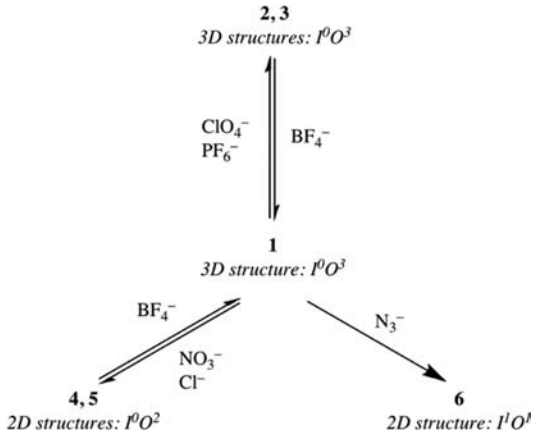

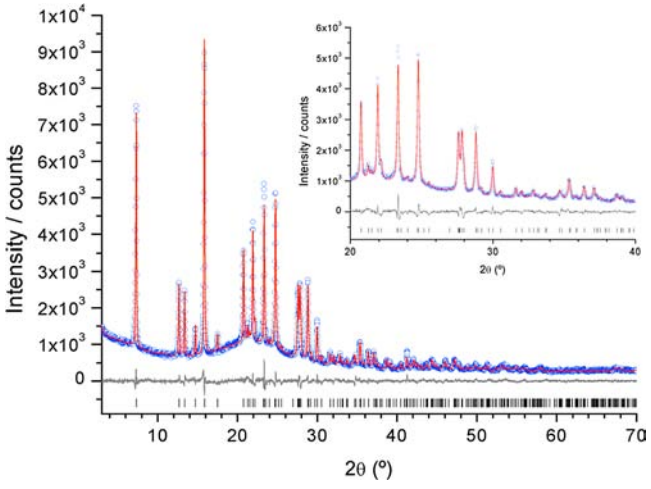

Figure 3. Observed (blue) and calculated (red) profiles and difference plots ($I_{obs} - I_{calcd}$; gray) of the Rietveld refinement of compound **6** (2θ range 3.0−70.0°; maximum resolution 1.34 Å).

plane, the $S = {}^1/_2$ 2D quadratic layer antiferromagnet model has been used to fit the magnetic data.[29] This model reproduces very satisfactorily the observed behavior of both compounds in the whole temperature range with $g = 2.18$ and $J = -0.16$ cm^{-1} (for **4**) and $g = 2.18$ and $J = -2.9$ cm^{-1} (for **5**) (solid lines in Figure 5b,c, with the Hamiltonian written as $H = -J\sum S_iS_{i+1}$).

Compound **6** presents a completely different magnetic behavior with an increase in χ_mT as the temperature is decreased, indicating the presence of predominant ferromagnetic interactions between the Cu^{II} ions. At very low temperatures, there is a decrease in χ_mT that may be attributed in a first approach to the presence of weaker antiferromagnetic interactions. Since the structure of compound **6** shows the presence of two kinds of bridges, *anti*-btix and asymmetric $\mu_{1,1'}$-N_3 bridges, we can assume that the observed ferromagnetic coupling is due to asymmetric $\mu_{1,1'}$-N_3 bridges, whereas the weaker antiferromagnetic coupling is due to the presence of *anti*-btix bridges. The structure of compound **6** shows that asymmetric $\mu_{1,1'}$-N_3 bridges form regular Cu^{II} chains that are further connected through the *anti*-btix ligands, so we have used a simple regular ferromagnetic chain model (J)[30] with interchain interactions (zj, with $z = 2$) also modeled with the molecular-field approximation. This model reproduces very satisfactorily the magnetic properties of compound **6** in the whole temperature range, including the maximum at very low

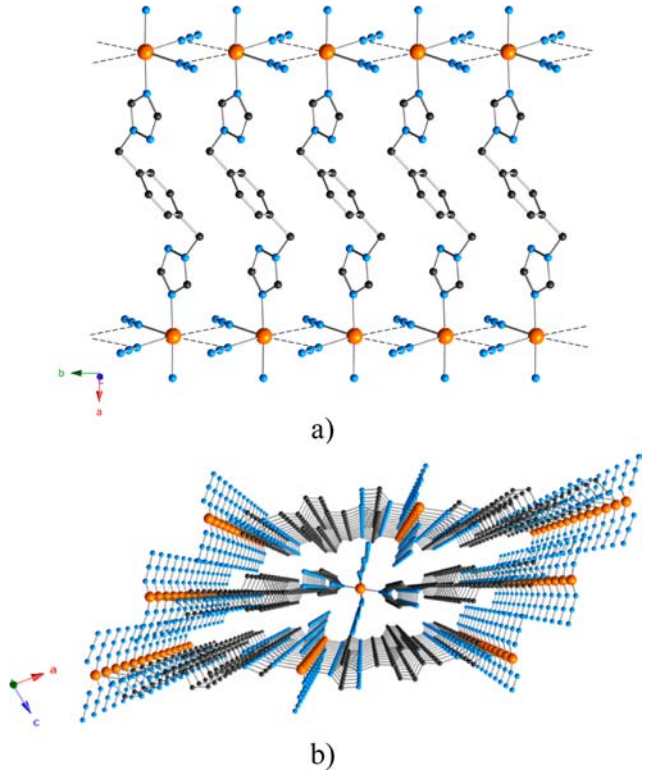

Figure 4. (a) 1D azido-bridged chains connected by *anti*-btix ligands showing the octahedral environment of the Cu^{II} centers in **6**. (b) 2D layers viewed along the *b* axis. Copper, nitrogen, and carbon atoms are colored orange, blue, and black, respectively; hydrogen atoms have been omitted for clarity.

temperatures, with $g = 2.21$, $J = 5.9$ cm^{-1}, and $j = -0.2$ cm^{-1} (solid line in Figure 5d, with the Hamiltonian written as $H = -J\Sigma S_iS_{i+1}$). As expected, the ferromagnetic coupling through the azido ligand is stronger than the weak antiferromagnetic interchain interactions through the btix one.

Although not very usual, the ferromagnetic coupling observed through the asymmetric $\mu_{1,1'}$-N_3 bridge can be well explained with the predictions based on density functional theory calculations performed for these kinds of asymmetric double bridges.[31] These calculations show that in double-asymmetric $\mu_{1,1'}$-N_3 bridges the main parameter determining the sign and strength of the magnetic coupling is the long Cu−N bond length. The coupling is usually weak and antiferromagnetic when this long Cu−N bond is below ca. 2.8 Å but it may be ferromagnetic for Cu−N bond lengths above ca. 2.8 Å, as observed in compound **6**, where this long Cu−N distance is 2.886(10) Å.

EPR. The powder X-band EPR spectra of **1** at room temperature (Figure 6a) displays a slightly axially distorted spectrum with a main narrow feature with a peak-to-peak line width of ca. 70 G at ca. 3300 G (perpendicular component at $g = 2.06$) and a weak and broad signal at ca. 2950 G (parallel component at $g \approx 2.29$, giving an average $\langle g \rangle = 2.14$, very close to the value found in the susceptibility measurements). These results support the tetragonally distorted coordination site and indicate that the unpaired electron on the Cu^{II} ion is located in the $x^2 - y^2$ d-type orbital, located in the equatorial CuN_4 plane.

Compound **6** presents a more complex EPR spectrum than compound **1** (Figure 6b). Thus, the EPR of **6** shows three very close signals at room temperature centered at ca. 3250 G ($g \approx$

dx.doi.org/10.1021/ic302066e | *Inorg. Chem.* 2012, 51, 12938−12947

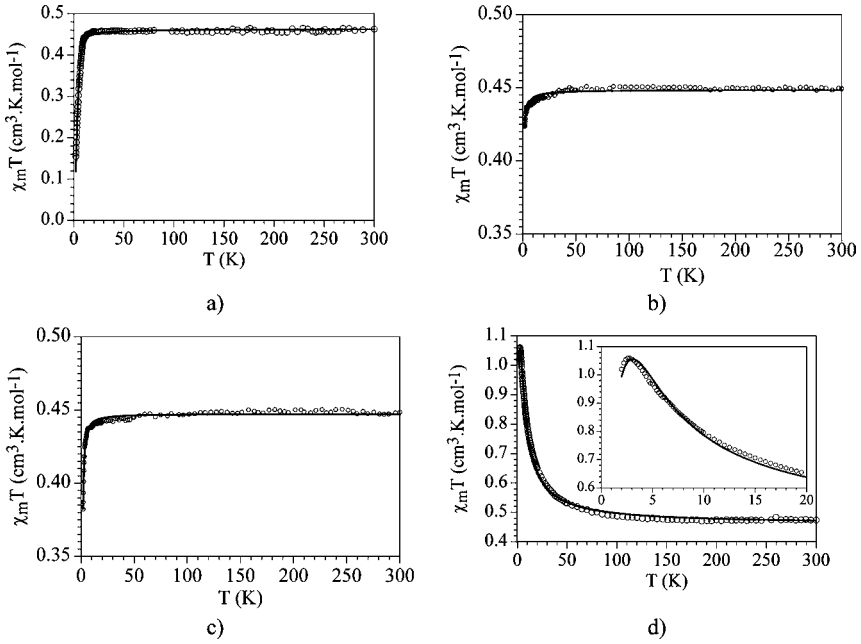

Figure 5. Thermal variation of the $\chi_m T$ product per Cu^{II} ion for compounds **1** (a), **4** (b), **5** (c), and **6** (d). Solid lines show the best fit to the models (see the text).

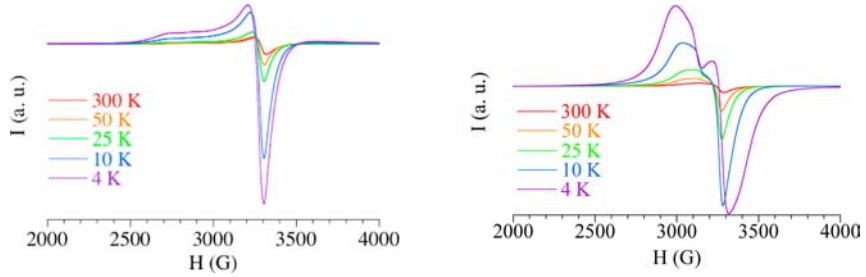

Figure 6. X-band EPR spectra at different temperatures for compounds **1** (left) and **6** (right).

2.08) that increase in intensity and split at low temperatures, leading to a *g* shift. The rhombic signal suggests a lower symmetry of the Cu^{II} site. However, the splitting of the three signals is not only due to the expected narrowing of the signals as the temperature is decreased but rather due to a shift of the two extreme components toward lower and higher fields in each case. Clearly, such behavior does not correspond to isolated Cu^{II} sites but rather to that of the low-dimensional exchange-coupled lattice formed in this case.

DISCUSSION

The use of the flexible ligand btix permits the synthesis of molecule-based materials with dynamic behavior in the solid state.[25] This ligand can adopt two different conformations, syn and anti, because of the presence of methylene groups between the triazole and benzene rings,[26] and both conformations are found in compound **1**. The presence of a weakly coordinated BF_4^- anion in compound **1**, together with the insolubility of this polymer in common organic solvents (and water), prompted us to explore whether substitution of this anion could lead to a dynamic response of the material, which could modify the magnetic properties. In addition, this process can be facilitated by the ligand btix, which provides the necessary flexibility for the anion exchange to occur given that this coordination polymer is nonporous. However, it must be noted that this anion exchange could also be a solvent-mediated process, as proposed by Khlobystov and co-workers,[32] who have shown that the degree of reversibility of some solvent-induced anion-exchange transformations is determined by the ratio of the solubility product constants for the starting and resulting complexes.

Compound **1** consists of a neutral 3D network with a very unusual coordination of BF_4^- anions and with the btix ligand in two different conformations, syn and anti. Immersion in 3 M solutions of $NaPF_6$ or $NaClO_4$ produces an anion exchange in the solids, as confirmed by FT-IR, with retention of the crystal structure. Thus, the ligands retain their original conformation (see Figure 7). However, upon exposure to NO_3^- and Cl^- anions, the anion exchange induces a conformational switch of half of the btix ligands from syn to anti conformation, with the formation of a neutral 2D grid with (4,4) topology (see Figure 7). This transformation requires a rearrangement in the metal environment and implies the cleavage of coordination bonds between Cu^{II} ions and btix ligands, followed by rotation of the btix ligand through the methylene groups to adopt the anti conformation and subsequent re-formation of the Cu−N bonds. The most remarkable anion-exchange process is the transformation **1** → **6**, which modifies enormously the connectivity of the metal centers. When crystalline solid **1** was immersed in 3 M NaN_3 aqueous solutions, a remarkable color change from purple to green was instantly observed.

dx.doi.org/10.1021/ic302066e | *Inorg. Chem.* 2012, 51, 12938−12947

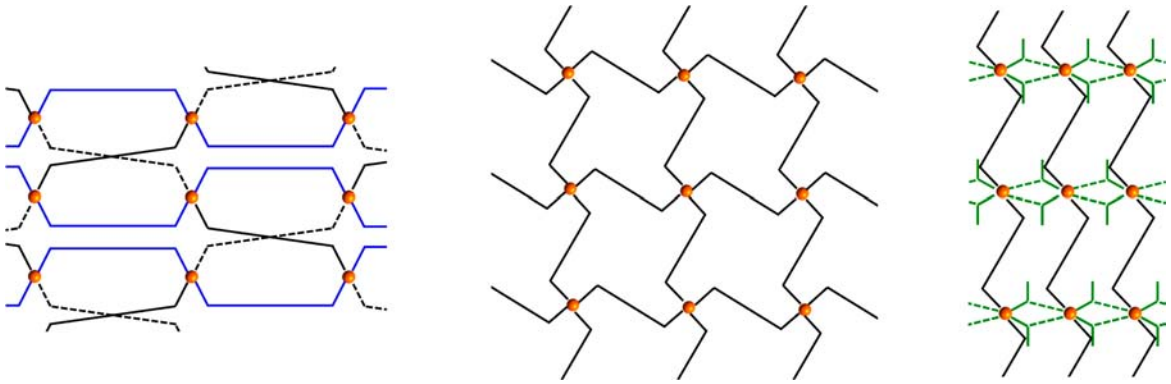

Figure 7. Schematic representation of the three different categories of coordination polymers with different conformations of the organic btix ligand: (a) 3D network of compounds **1**−**3** with I^0O^3 connectivity with half of the btix ligands in the anti conformation (represented in black) and half in the syn conformation (represented in blue); (b) 2D network of compounds **4** and **5** with I^0O^2 connectivity with all of the btix ligands in the anti conformation; (c) 2D network of compound **6** with I^1O^1 connectivity with all of the btix ligands in the anti conformation (green lines represent the inorganic connectivity).

During this process, a drastic rearrangement of the network occurs because of exchange of the BF_4^- anions by N_3^- anions, accompanied by the loss of one coordinated btix ligand which is transferred to the aqueous solution, whereas the remaining btix ligand remains in the anti conformation. This elimination of an organic ligand during anion exchange is not unprecedented and has recently been reported.[33] Nevertheless, given the change in the Cu/btix ratio between **1** and **6** and the gross structural changes, it is likely that the reaction occurs via dissolution of the precursor before (or simultaneously with) crystallization of the final product, analogous to that demonstrated for some anion-exchange reactions involving crystalline solids.[32] The anion-exchange process is clearly evidenced in the IR study by detecting the disappearance of a strong IR peak at 1084 cm^{-1} (characteristic of the BF_4^- anion) in compound **1** accompanied by the appearance of two new strong peaks at 2046 and 2025 cm^{-1} (characteristic of the N_3^- anion) in the exchanged compound **6**. These peaks appear at lower frequencies than is usually expected for $\mu_{1,1'}$-1,1-azido bridging anions, in agreement with the highly asymmetrical nature of the azido bridge in the polymer.[34] The appearance of two bands should be related to the presence of two crystallographically independent N_3^- anions. However, only one type of azido can be found in the crystal structure of **6**. This suggests the existence of some degree of disorder in the azido bridging groups that is impossible to model in the Rietveld refinement from powder data. Interestingly, when a mixture of anions is used, the N_3^- anion is exclusively trapped by compound **1** in the presence of ClO_4^-, PF_6^-, NO_3^-, and Cl^-, as is clearly demonstrated by the immediate transformation of the original violet crystals to green crystals in a quantitative manner. Thus, this permits the detection of NaN_3 from an aqueous solution in the presence of other anions, which can be of great use for the elimination of toxic azido ligands.[35] In this sense, the highly efficient and complete replacement of the anionic species implies that 2 mol of NaN_3 can be eliminated per 1 mol of compound **1**. Furthermore, compounds **2**−**5** can be transformed into **6** upon immersion of these coordination polymers into a NaN_3 solution.

The different categories of coordination polymers upon anion exchange are clearly differentiated following the classification introduced by Cheetham et al.,[4k] where coordination polymers are categorized by the dimensionality of their inorganic and organic connectivity as I^mO^n, where "I" and "O" refer to the connectivity through the inorganic and organic ligands, respectively, and "*m*" and "*n*" refer to the dimensionality of each type of connectivity. Compound **1** falls in the category of I^0O^3, quite common in MOFs. Upon exchange with ClO_4^- (**2**) and PF_6^- (**3**), the dimensionality of the exchanged coordination polymers is maintained as I^0O^3. However, anion exchange to NO_3^- (**4**) and Cl^- (**5**) produces a change in the connectivity to I^0O^2; i.e., the dimensionality is reduced from 3D to 2D without involvement of the inorganic ligand. Furthermore, a conformational change of half of the ligands takes place during anion exchange because all btix ligands are found in the anti configuration for compounds **4** and **5**. Interestingly, upon exchange to N_3^- (**6**), the rare I^1O^1 topology is found, combining organic and inorganic ligands in the connectivity of the coordination polymer. This clearly shows that the crystal structures of these materials, and therefore their magnetic properties, are extremely sensitive to the nature of the anion used in the exchange. Thus, this crystal engineering approach is not only aesthetic but also functional because it allows one to design new magnetic coordination polymers that could have applicability as anion exchangers or for anion trapping. In addition, the presence of a flexible crystalline lattice opens up the possibility for introducing anions of different sizes, thus overcoming the problem of robust MOFs whose pore sizes limit the dimension of the species that can enter.

Although the number of used anions is limited and it is difficult to extract a definite conclusion, we have tried to rationalize the response of the crystalline lattice toward the different anions. It seems that modification of the crystal structures upon anion exchange might be related to the coordinating ability of the different anions.[22] Thus, exchange of the weak coordinating ligand BF_4^- ($a = -1.1$) by weak coordinating ligands ClO_4^- ($a = -0.6$) or PF_6^- ($a = -1.6$) does not produce any structural change and the original structure is maintained. However, when more coordinating anions are used, such as Cl^- ($a = 1.3$) and NO_3^- ($a = 0.1$), the structure is slightly modified. Finally, when a highly coordinating ligand such as N_3^- ($a = 2.1$) is used, the structure is fully changed because of the strong coordinating tendency of the N_3^- ligand. It seems that the geometry of the anions does not play a significant role in the structural modification of the network.

This difference in coordination ability might also be related with the reversibility of the anion exchange. The less

coordinating anions, ClO_4^- and PF_6^-, are quantitatively exchanged with BF_4^- and, therefore, coordination polymers **2** and **3** easily reconvert into **1**. This idea implies that the more coordinating anions Cl^-, NO_3^-, and N_3^- should not be quantitatively exchanged with BF_4^-, as is observed in the case of compounds **4** and **6**. However, Cl^- anions are exchanged with BF_4^-, which could be due to the smaller size of the Cl^- anion (which would favor its exit through the channels) compared with the NO_3^- anion. However, this could also be due to differences in the solubility of the coordination polymers.[32]

CONCLUSIONS

In conclusion, in this work we have shown that the nonporous coordination polymer $[Cu(btix)_2]_n^{2n+}$ displays dynamic transformations in the solid state when the coordinated BF_4^- anion of the starting material is exchanged with other inorganic monoanions. In fact, this coordination polymer reversibly exchanges BF_4^- with PF_6^- and ClO_4^-, maintaining its structure, or with NO_3^- and Cl^-, modifying the dimensionality of the network because of changes in the conformation of the flexible organic ligand. Moreover, this coordination polymer is capable of irreversibly converting into $[Cu(btix)(N_3)_2]$ in the crystalline state when it is immersed in an aqueous solution of NaN_3, producing a change of color of the solid. This conversion undergoes severe structural changes that affect the magnetic properties of the coordination polymers because of changes in the connectivity between the metal centers. Notice that the rapid change of color in response to the presence of azide anions provides potential applications as chemical sensors. The flexibility of the lattice presents the additional advantage of overcoming the size limit found in robust frameworks. Thus, the MOFs presented here describe an approach based on crystal engineering that can be exploited to design dynamic magnetic nanomaterials that permit the exchange of anionic species of different sizes and the selective detection and trapping of toxic azide anions.

ASSOCIATED CONTENT

Supporting Information

X-ray crystallographic data in CIF format, EA for **1**−**6**, unit cell parameters from Pawley refinements for **1**−**5**, and IR spectra. This material is available free of charge via the Internet at http://pubs.acs.org.

AUTHOR INFORMATION

Corresponding Author

*E-mail: guillermo.minguez@uv.es.

Notes

The authors declare no competing financial interest.

ACKNOWLEDGMENTS

The work has been supported by the European Union (Advanced ERC Grant SPINMOL and FP7 Project HINTS), the Spanish Ministerio Economía de y Competitividad, MINECO (Project Consolider-Ingenio in Molecular Nanoscience, CSD2007-00010, and Projects MAT2007-61584, MAT2011-22785, and CTQ2011-26507 cofinanced by FEDER), and the Generalitat Valenciana (Prometeo and ISIC Programs). M.G.-M. thanks MINECO for a predoctoral grant. We also acknowledge J. M. Martínez-Agudo and G. Agustí (University of Valencia) for their help with the magnetic and EPR measurements.

REFERENCES

(1) Kahn, O.; Martinez, C. J. *Science* **1998**, *279*, 44.
(2) (a) Robson, R. *J. Chem. Soc., Dalton Trans.* **2000**, 3735. (b) Hoskins, B. F.; Robson, R. *J. Am. Chem. Soc.* **1989**, *111*, 5962. (c) Blake, A. J.; Champness, N. R.; Hubberstey, P.; Li, W.-S.; Withersby, M. A.; Schröder, M. *Coord. Chem. Rev.* **1999**, *183*, 117.
(3) See the recent themed issues on MOFs: (a) *Chem. Soc. Rev.* **2009**, *38*, 1201−1508. (b) *Chem. Rev.* **2012**, *112*, 673−1268.
(4) For reviews on MOFs and coordination polymers, see: (a) Rowsell, J. L. C.; Yaghi, O. M. *Microporous Mesoporous Mater.* **2004**, *73*, 3. (b) Kitagawa, S.; Kitaura, R.; Noro, S.-i. *Angew. Chem., Int. Ed.* **2004**, *43*, 2334. (c) Suh, M. P.; Cheon, Y. E.; Lee, E. Y. *Coord. Chem. Rev.* **2008**, *252*, 1007. (d) Férey, G. *Chem. Soc. Rev.* **2008**, *37*, 191. (e) James, S. L. *Chem. Soc. Rev.* **2003**, *32*, 276. (f) Janiak, C. *Dalton Trans.* **2003**, 2781. (g) Bradshaw, D.; Claridge, J. B.; Cussen, E. J.; Prior, T. J.; Rosseinsky, M. J. *Acc. Chem. Res.* **2005**, *38*, 273. (h) Cohen, S. M. *Chem. Sci.* **2010**, *1*, 32. (i) Zhao, D.; Timmons, D. J.; Yuan, D.; Zhou, H.-C. *Acc. Chem. Res.* **2011**, *44*, 123. (j) Dincă, M.; Long, J. R. *Angew. Chem., Int. Ed.* **2008**, *47*, 6766. (k) Cheetham, A. K.; Rao, C. N. R.; Feller, R. K. *Chem. Commun.* **2006**, 4780. (l) Champness, N. R. *Dalton Trans.* **2011**, *40*, 10311. (m) Brammer, L. *Chem. Soc. Rev.* **2004**, *33*, 476. (n) Medina, M. E.; Platero-Prats, A. E.; Snejko, N.; Rojas, A.; Monge, A.; Gándara, F.; Gutiérrez-Puebla, E.; Camblor, M. A. *Adv. Mater.* **2011**, *23*, 5283. (o) Phan, A.; Doonan, C. J.; Uribe-Romo, F. J.; Knobler, C. B.; O'Keefe, M.; Yaghi, O. M. *Acc. Chem. Res.* **2010**, *43*, 58.
(5) Coronado, E.; Mínguez Espallargas, G. *Chem. Soc. Rev.* **2013**, DOI:10.1039/C2CS35278H
(6) (a) Gütlich, P.; Hauser, A.; Spiering, H. *Angew. Chem., Int. Ed.* **1994**, *33*, 2024. (b) Sato, O.; Iyoda, T.; Fujishima, A.; Hashimoto, K. *Science* **1996**, *272*, 704. (c) Coronado, E.; Giménez-López, M. C.; Levchenko, G.; Romero, F. M.; García-Baonza, V.; Milner, A.; Paz-Pasternak, M. *J. Am. Chem. Soc.* **2005**, *127*, 4580. (d) Coronado, E.; Giménez-López, M. C.; Korzeniak, T.; Levchenko, G.; Romero, F. M.; Segura, A.; García-Baonza, V.; Cezar, J. C.; de Groot, F. H. F.; Milner, A.; Paz-Pasternak, M. *J. Am. Chem. Soc.* **2008**, *130*, 15519. (e) Egan, L.; Kamenev, K.; Papanikolaou, D.; Takabayashi, Y.; Margadonna, S. *J. Am. Chem. Soc.* **2006**, *128*, 6034.
(7) (a) Coronado, E.; Giménez-Marqués, M.; Mínguez Espallargas, G.; Brammer, L. *Nat. Commun.* **2012**, *3*, 828. (b) Navarro, J. A. R.; Barea, E.; Rodríguez-Diéguez, A.; Salas, J. M.; Ania, C. O.; Parra, J. B.; Masciocchi, N.; Galli, S.; Sironi, A. *J. Am. Chem. Soc.* **2008**, *130*, 3978. (c) Ohkoshi, S.; Arai, K.; Sato, Y.; Hashimoto, K. *Nat. Mater.* **2004**, *3*, 857. (d) Zhang, Y.-J.; Liu, T.; Kanegawa, S.; Sato, O. *J. Am. Chem. Soc.* **2009**, *131*, 7942. (e) Pinkowicz, D.; Podgajny, R.; Gaweł, B.; Nitek, W.; Łasocha, W.; Oszajca, M.; Czapla, M.; Makarewicz, M.; Bałanda, M.; Sieklucka, B. *Angew. Chem., Int. Ed.* **2011**, *50*, 3973. (f) Kurmoo, M.; Kumagai, H.; Chapman, K. W.; Kepert, C. J. *Chem. Commun.* **2005**, 3012.
(8) (a) Cohen, S. R. *Chem. Rev.* **2012**, *112*, 970. (b) Wang, Z.; Cohen, S. R. *Chem. Soc. Rev.* **2009**, *38*, 1315. (c) Ingleson, M. J.; Perez Barrio, J.; Guilbaud, J.-B.; Khymyak, Y. Z.; Rosseinsky, M. J. *Chem. Commun.* **2008**, 2680. (d) Burrows, A. D.; Frost, C. D.; Mahon, M. F.; Richardson, C. *Angew. Chem., Int. Ed.* **2008**, *47*, 8482. (e) Tanabe, K. K.; Wang, Z.; Cohen, S. R. *J. Am. Chem. Soc.* **2008**, *130*, 8508. (f) Nagai, A.; Guo, Z.; Feng, X.; Jin, S.; Chen, X.; Ding, X.; Jiang, D. *Nat. Commun.* **2011**, *2*, 536.
(9) (a) Bradshaw, D.; Warren, J. E.; Rosseinsky, M. J. *Science* **2007**, *315*, 977. (b) Beauvais, L. G.; Shores, M. P.; Long, J. R. *J. Am. Chem. Soc.* **2000**, *122*, 2763. (c) Wu, C.-D.; Hu, A.; Zhang, L.; Lin, W. *J. Am. Chem. Soc.* **2005**, *127*, 8940. (d) Mínguez Espallargas, G.; Brammer, L.; van de Streek, J.; Shankland, K.; Florence, A. J.; Adams, H. *J. Am. Chem. Soc.* **2006**, *128*, 9584. (e) Mínguez Espallargas, G.; Hippler, M.; Florence, A. J.; Fernandes, P.; van de Streek, J.; Brunelli, M.; David, W. I. F.; Shankland, K.; Brammer, L. *J. Am. Chem. Soc.* **2007**, *129*, 15606. (f) Mínguez Espallargas, G.; van de Streek, J.; Fernandes, P.; Florence, A. J.; Brunelli, M.; Shankland, K.; Brammer, L. *Angew. Chem., Int. Ed.* **2010**, *49*, 8892. (g) Libri, S.; Mahler, M.; Mínguez Espallargas, G.; Singh, D. C. N. G.; Soleimannejad, J.; Adams, H.; Burgard, M. D.;

Rath, N. P.; Brunelli, M.; Brammer, L. *Angew. Chem., Int. Ed.* **2008**, *47*, 1693.
(10) (a) Hoskins, B. F.; Robson, R. *J. Am. Chem. Soc.* **1990**, *112*, 1546. (b) Yaghi, O. M.; Li, H. *J. Am. Chem. Soc.* **1995**, *117*, 10401. (c) Yaghi, O. M.; Li, H. *J. Am. Chem. Soc.* **1996**, *118*, 295. (d) Noro, S.-i.; Kitaura, R.; Kondo, M.; Kitagawa, S.; Ishii, T.; Matsuzaka, H.; Yamashita, M. *J. Am. Chem. Soc.* **2002**, *124*, 2568. (e) Carlucci, L.; Ciani, G.; Maggini, S.; Proserpio, D. M.; Visconti, M. *Chem.—Eur. J.* **2010**, *16*, 12328. (f) Aijaz, A.; Lama, P.; Bharadwaj, P. K. *Inorg. Chem.* **2010**, *49*, 5883. (g) Custelcean, R.; Moyer, B. A. *Eur. J. Inorg. Chem.* **2007**, 1321. (h) Fei, H.; Bresler, M. R.; Oliver, S. R. J. *J. Am. Chem. Soc.* **2011**, *133*, 11110. (i) Safarifard, V.; Morsali, A. *CrystEngComm* **2011**, *13*, 4817. (j) Fu, J.; Li, H.; Mu, Y.; Hou, H.; Fan, Y. *Chem. Commun.* **2011**, *47*, 5271. (k) Du, M.; Guo, Y.-M.; Chen, S.-T.; Bu, X.-H.; Batten, S. R.; Ribas, J.; Kitagawa, S. *Inorg. Chem.* **2004**, *43*, 1287. (l) Qiu, Y.; Liu, Z.; Li, Y.; Deng, H.; Zeng, R.; Zeller, M. *Inorg. Chem.* **2008**, *47*, 5122. (m) Sarkar, M.; Biradha, K. *Cryst. Growth Des.* **2006**, *6*, 1742. (n) Tzeng, B.-C.; Chiu, T.-H.; Chen, B.-S.; Lee, G.-H. *Chem.—Eur. J.* **2008**, *14*, 5237.
(11) (a) An, J.; Rosi, N. L. *J. Am. Chem. Soc.* **2010**, *132*, 5578. (b) Calleja, G.; Botas, J. A.; Sánchez-Sánchez, M.; Orcajo, M. G. *Int. J. Hydrogen Energy* **2010**, *35*, 9916.
(12) Beer, P. D.; Gale, P. A. *Angew. Chem., Int. Ed.* **2001**, *40*, 486.
(13) (a) Min, K. S.; Suh, M. P. *J. Am. Chem. Soc.* **2000**, *122*, 6834. (b) Noro, S.-i.; Tanaka, D.; Sakamoto, H.; Shimomura, S.; Kitagawa, S.; Takeda, S.; Uemura, K.; Kita, H.; Akutagawa, T.; Nakamura, T. *Chem. Mater.* **2009**, *21*, 3346. (c) Noro, S.-i.; Akutagawa, T.; Nakamura, T. *Chem. Commun.* **2010**, *46*, 3134.
(14) Meng, X.; Song, Y.; Hou, H.; Han, H.; Xiao, B.; Fan, Y.; Zhu, Y. *Inorg. Chem.* **2004**, *43*, 3528.
(15) Sheldrick, G. M. *Acta Crystallogr., Sect. A: Found. Crystallogr.* **2008**, *64*, 112.
(16) Coelho, A. A. *TOPAS*, version 4.1; Academic Press: New York, 2007; http://www.topas-academic.net.
(17) Pawley, G. S. *J. Appl. Crystallogr.* **1981**, *14*, 357.
(18) David, W. I. F.; Shankland, K.; Shankland, N. *Chem. Commun.* **1998**, 931.
(19) David, W. I. F.; Shankland, K.; van de Streek, J.; Pidcock, E.; Motherwell, S.; Cole, J. C. *J. Appl. Crystallogr.* **2006**, *39*, 910.
(20) Rietveld, H. M. *J. Appl. Crystallogr.* **1969**, *2*, 65.
(21) Ding, B.; Liu, Y.-Y.; Huang, Y.-Q.; Shi, W.; Cheng, P.; Liao, D.-Z.; Yan, S.-P. *Cryst. Growth Des.* **2009**, *9*, 593.
(22) Díaz-Torres, R.; Alvarez, S. *Dalton Trans.* **2011**, *40*, 10742.
(23) a (transition metal) is defined as $\log(c + s)/u$,[22] where c, s, and u are the number of structures with the group coordinated, semi-coordinated, and uncoordinated, respectively. A positive value of a indicates that the group has a higher chance to coordinate to a transition-metal atom than to remaining uncoordinated group in its presence (the larger the positive value of a, the greater its coordinating ability). On the other hand, large negative values of a indicate a poor tendency to coordinate).
(24) Nakamoto, K. *Infrared and Raman Spectra of Inorganic and Coordination Compounds*, 4th ed.; John Wiley & Sons: New York, 1986.
(25) Coronado, E.; Giménez-Marqués, M.; Mínguez Espallargas, G. *Inorg. Chem.* **2012**, *51*, 4403.
(26) (a) Liu, K.; Shi, W.; Cheng, P. *Dalton Trans.* **2011**, *40*, 8475. (b) Li, B.; Peng, Y.; Li, B.; Zhang, Y. *Chem. Commun.* **2005**, 2333. (c) Meng, X.; Liu, Y.; Song, Y.; Hou, H.; Fan, Y.; Zhu, Y. *Inorg. Chim. Acta* **2005**, *358*, 3024. (d) Li, B.; Peng, Y.; Liu, X.; Li, B.; Zhang, Y. *J. Mol. Struct.* **2005**, *741*, 235. (e) Peng, Y.-F.; Ge, H.-Y.; Li, B.-Z.; Li, B.-L.; Zhang, Y. *Cryst. Growth Des.* **2006**, *16*, 994. (f) Du, J.-L.; Hu, T.-L.; Zhang, S.-M.; Zeng, Y.-F.; Bu, X.-H. *CrystEngComm* **2008**, *10*, 1866. (g) Chen, Y.; Zhang, S.-Y.; Zhao, X.-Q.; Zhang, J.-J.; Shi, W.; Cheng, P. *Inorg. Chem. Commun.* **2010**, *13*, 699. (h) Zhang, S.-Y.; Zhang, Z.-J.; Shi, W.; Zhao, B.; Cheng, P.; Liao, D.-Z.; Yan, S.-P. *Dalton Trans.* **2011**, *40*, 7993.
(27) Brown, D. B.; Donner, J. A.; Hall, J. W.; Wilson, S. R.; Wilson, R. B.; Hodgson, D. J.; Hatfield, W. E. *Inorg. Chem.* **1979**, *18*, 2635.
(28) O'Connor, C. J. *Prog. Inorg. Chem.* **1982**, *29*, 203.
(29) Lines, M. E. *J. Phys. Chem. Solids* **1970**, *31*, 101.
(30) Baker, G. A., Jr.; Rushbrooke, G. S.; Gilbert, H. E. *Phys. Rev.* **1964**, *135*, A1272.
(31) Triki, S.; Gómez-García, C. J.; Ruiz, E.; Sala-Pala, J. *Inorg. Chem.* **2005**, *44*, 5501.
(32) (a) Khlobystov, A. N.; Champness, N. R.; Roberts, C. J.; Tendler, S. J. B.; Thompson, C.; Schröder, M. *CrystEngComm* **2002**, *4*, 426. (b) Cui, X.; Khlobystov, A. N.; Chen, X.; Marsh, D. H.; Blake, A. J.; Lewis, W.; Champness, N. R.; Roberts, C. J.; Schröder, M. *Chem.—Eur. J.* **2009**, *15*, 8861.
(33) Supriya, S.; Das, S. K. *Chem. Commun.* **2011**, *47*, 2062.
(34) (a) Ray, M. S.; Ghosh, A.; Bhattacharya, R.; Mukhopadhyay, G.; Drew, M. G. B.; Ribas, J. *Dalton Trans.* **2004**, 252. (b) De Munno, G.; Lombardi, M. G.; Julve, M.; Lloret, F.; Faus, J. *Inorg. Chim. Acta* **1998**, *282*, 82.
(35) (a) Suzuki, A.; Ivandini, T. A.; Kamiyac, A.; Nomurad, S.; Yamanuki, I.; Matsumoto, K.; Fujishima, A.; Einaga, Y. *Sens. Actuators, B* **2007**, *120*, 500. (b) Xu, J.; Swain, G. M. *Anal. Chem.* **1998**, *70*, 1502. (c) Szabados, T.; Dul, C.; Majtényi, K.; Hargitai, J.; Pénzes, Z.; Urbanics, R. *Behav. Brain Res.* **2004**, *154*, 31. (d) Dalmia, A.; Savinell, R. F.; Liu, C. C. *J. Electrochem. Soc.* **1996**, *143*, 1827. (e) Sezginturk, M. K.; Göktuğ, T.; Dinçkaya, E. *Biosens. Bioelectron.* **2005**, *21*, 684.